# The development of chemical tools to study the interplay of ubiquitination and ADPribosylation

Kloet, M.S.

# Chapter 8

## Summary & Future directions

## Summary

Ub$^{ADPr}$ is a combination of the two post-translational modifications (PTMs) Adenosine diphosphate ribose (ADPr) and ubiquitin (Ub) covalently attached to each other. Ub$^{ADPr}$ has gained interest as key intermediate in the phosphoribosyl (PR)-ubiquitination pathway utilized by the Legionella bacterium to gain local control of the host Ub system. Furthermore, examples of mammalian enzymes forming Ub$^{ADPr}$ are emerging, highlighted by the identification of the Deltex RING E3 ligase family. Tools to study formation or signaling of Ub$^{ADPr}$ are scarce, mainly attributed to synthetic challenges associated with covalently linking and deprotecting Ub$^{ADPr}$. This thesis focuses on the synthesis and application of Ub$^{ADPr}$-tools and this final chapter summarizes (**Fig. 1**) the results and outlines promising future directions.

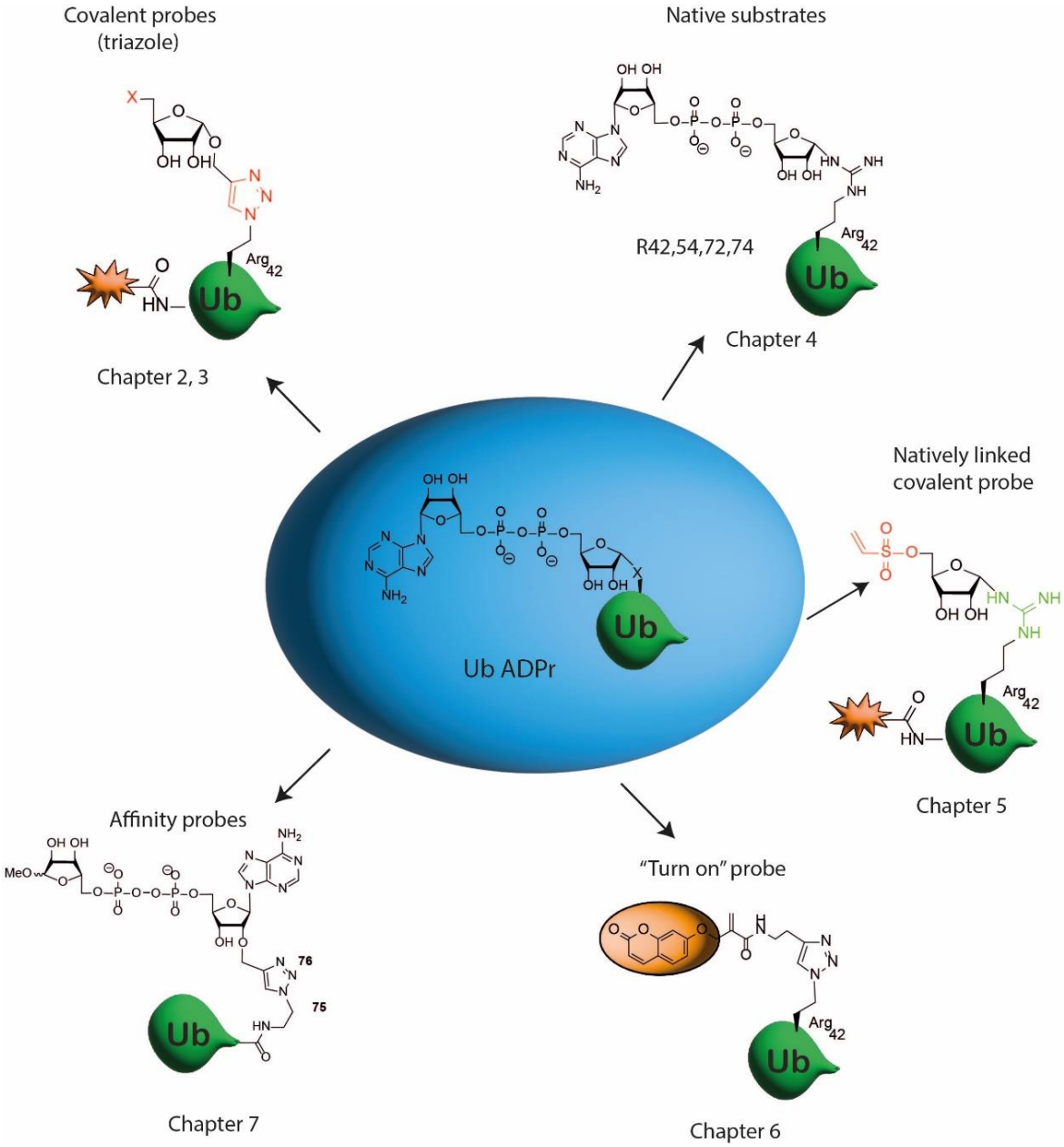

**Fig. 1**. Schematic overview of the work presented in this thesis.

**Chapter 1** provides an overview of $Ub^{ADPr}$ in the context of the known biological pathways it plays a role in. The current status of chemical methodologies and biochemical assays to study enzymes related to $Ub^{ADPr}$ is discussed as well.

**Chapter 2** describes the development of phosphoribosyl ubiquitin mimics as probes to covalently capture Legionella effector enzymes. Synthesized ribosides equipped with a 5'-O warhead and 1'-O propargyl were conjugated to ubiquitin featuring an Arg42 to azido-homoalanine mutation using the copper-catalyzed azide-alkyne cycloaddition (CuAAC). Assessment of the probe library *in vitro* on recombinant DupA revealed that the probe based on the vinyl sulfonate warhead was able to most efficiently capture DupA covalently. Despite the initial goal of targeting a reactive active site His of DupA based on structural studies, the vinyl sulfonate probe unexpectedly reacted with Cys196, a residue in close proximity to the active site as evidenced by mass spectrometry and X-ray crystallography. Applying the hydrolytically-stable triazole-linked probe in a pulldown-proteomics experiment non-the-less enriched both DupA and DupB from Legionella-infected HEK293T lysate (**Fig. 2**). This outcome validated the applicability of the probe in a complex proteome. Moreover, the subset of mammalian proteins differing in enrichment upon infection could be monitored, of which PARP1 enrichment showed to be negatively influenced by the infection. Analyzing this interesting hit, it might be that Legionella inactivates PARP1 during infection as a mechanism to delay the immune response, as is similarly observed in the context of *Salmonella enterica* infection.[1] However, further research is required to substantiate this.

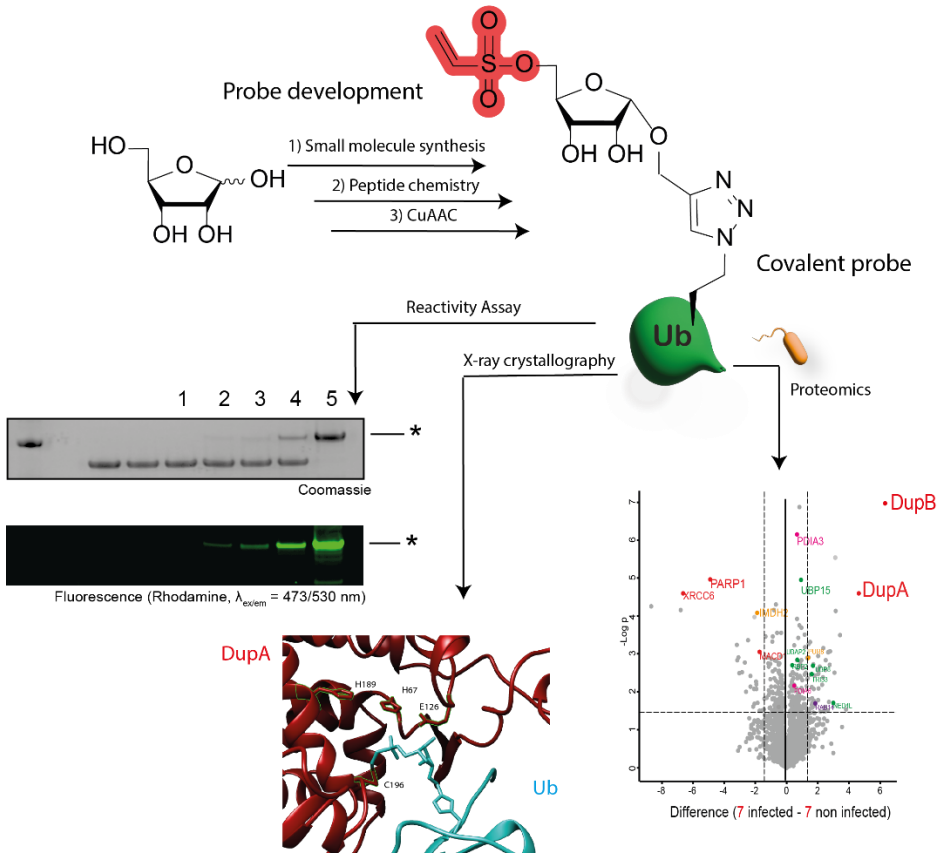

**Fig. 2**. Schematic overview of the work described in **chapter 2**.

While targeting a cysteine near the active site in DupA enabled the enrichment of DupA and DupB in lysates from Legionella-infected HEK293T cells, interest in developing a probe that binds to one of the active site histidine's in DupA remained. Histidine residues make up over 18%[2] of active site residues in proteins, but finding an electrophilic warhead that selectively targets this residue is challenging due to its moderate nucleophilicity and the potential for side reactivity of the warhead with more nucleophilic side chains of amino acids such as cysteine and lysine. Discovering a warhead selective for histidine would not only aid in the context of DupA targeting but could also be generally applied to other enzymes containing histidine in the active site. In **Chapter 3**, this goal was pursued by synthesizing a photoactivable probe to potentially induce a histidine selective reaction in the active site of DupA via photochemistry. The synthesis involved the installment of the photoactivatable pyridinium warhead at the primary alcohol of an alkyne equipped riboside and subsequently converting it into a phosphoribose ubiquitin mimicking probe via the CuAAC approach described in chapter 2. The photoactivation of the pyridinium warhead in the UV-B range has been documented to only target His and Trp residues.[3,4] Given that Trp is not present in the active site of DupA and previous findings suggest the pyridinium warhead does not react with Cys, we hypothesized this probe could circumvent Cys196 and react to one of the active site His residues in DupA. Gratifyingly, photoactivation of the pyridinium probe in the UVB-range (302 nm) crosslinked DupA and the phosphoribose mimicking probe covalently. However, moderate conversion was observed, along with presumed photo-degradation, as indicated by HRMS and SDS-PAGE. This was improved when incorporating glutathione (GSH) into the reaction mixture, as the additive demonstrated a protective effect on DupA and enhanced the conversion. To determine the binding site, mutagenesis of the active site residues was undertaken, and notably, variations in labeling were observed when crosslinking the probe to the mutants. Notably, compared to DupA wild-type, the His189 to Asn mutant shows reduced conversion, whereas all other mutants, including the Cys196 to Ala mutant, maintain similar reactivity toward the probe (**Fig. 3**). Overall, this preliminary data does not conclusively identify the binding site of the probe. Although probe reactivity decreases with the single His189 mutant, the double His67/His189 mutant shows labeling comparable to wild-type DupA. Given the presence of additional His residues not covered in this mutation study, it is possible that mutating a specific His residue may redirect the probe toward another His residue. However, conducting crosslinking in HEK cell lysate with the addition of DupA and the probe demonstrates the adaptability of this procedure to more complex biological systems and shows the potential of the probe to monitor Legionella effector enzymes involved in PR-ubiquitination in Legionella-infected cells.

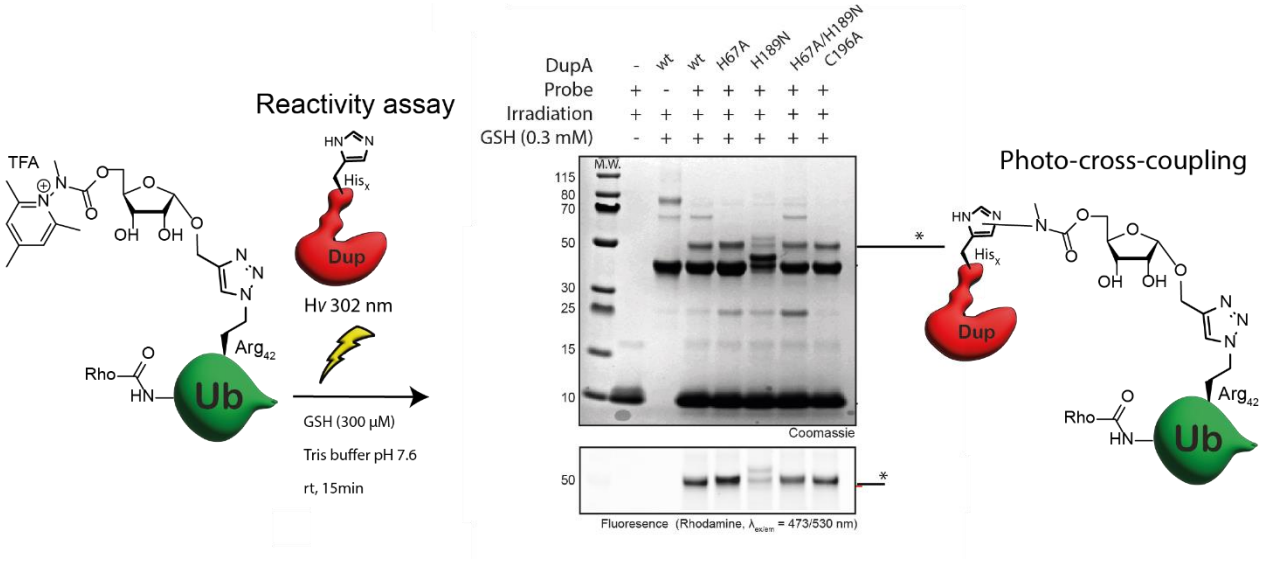


**Fig. 3**. Schematic summary of the work described in **Chapter 3**.

In **Chapter 4** we set out to develop a generally applicable methodology to synthesize natively Arg linked ADPr-ribosylated peptides and expand this to the full chemical synthesis of $^{Arg}Ub^{ADPr}$. The synthesis of Arg-ADPr peptides involved reacting an ornithine containing polypeptide on-resin with an α-linked isothiourea N-riboside, mediated by silver, resulting in the native guanidinium linkage. Subsequent phosphorus chemistry via previously established methods is used to built the ADPr moiety onto the ribosylated peptide. TFA-mediated deprotection and release of the resin successfully yielded well-defined Arg-ADPribosylated peptides and $Ub^{ADPr}$. The developed method was used to prepare all four $^{Arg}Ub$-regio-isomers (Arg-42, Arg-54, Arg-72 and Arg-74) marking the first examples of ADPr installed on synthetic proteins. Gratifyingly, the synthetic proteins were processed by Legionella enzymes and hence enabled to profile the activity and selectivity of *Legionella pneumophila* ligase- and hydrolase enzymes using the entire suite of $Ub^{ADPr}$ isomers (**Fig. 4**). While anomerization has been reported to occur under physiological conditions, the acid-mediated liberation to produce synthetic $Ub^{ADPr}$ might have contributed to the anomerization, resulting in a slower processing by Legionella effectors.

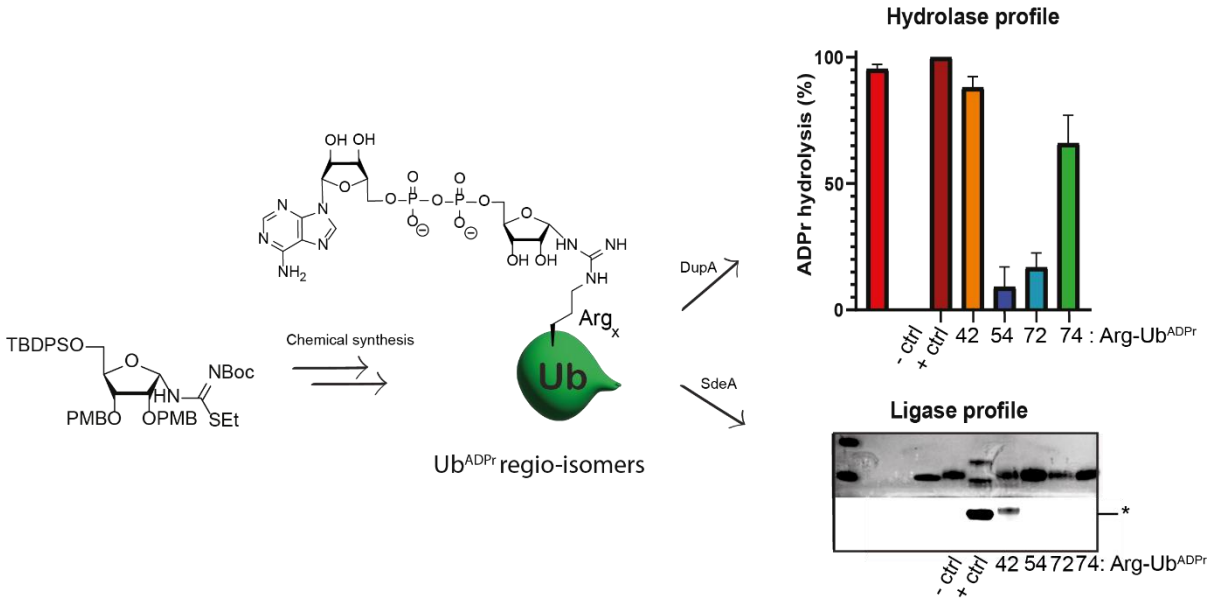


**Fig. 4**. Schematic overview of the work described in **Chapter 4**.

Equipped with a methodology to create the native arginine ADPr linkage, we aimed to expand the toolbox with natively linked variants (**Chapter 5**) of the probes developed in Chapter 2. The triazole linkage serves as arginine mimic and is well-tolerated by the Legionella effectors DupA and SdeA. However, Bio-Layer Interferometry (BLI) and auto-ubiquitination assays, which compared triazole-linked $Ub^{ADPr}$ to enzymatically produced natively-linked $Ub^{ADPr}$ as a substrate for SdeA and DupA, revealed a reduced affinity for the triazole-linked material.[5,6] Consequently, synthesizing native Arg-ribose linked probes and substrates holds the potential to improve enzyme-recognition and affinity of such material, although there is a potential of glycosidic bond hydrolysis in e.g. lysate by ADP-ribosyl hydrolase (ARH) activity. The native analogues of the fluorosulfonate and vinyl sulfonate probe were successfully synthesized by first installing the respective warheads on the primary alcohol of the α-linked isothiourea N-riboside, following conjugation to ubiquitin via the ornithine residue (**Chapter 5**). Both probes labeled DupA and SdeA on recombinant protein, albeit with a reduced reaction rate compared to their triazole derivatives (**Fig. 5**). This observation might be attributed to the previously described anomerization potentially occurring during the synthesis. The native vinyl sulfonate probe was subjected to a pulldown in Legionella infected HEK293T cell lysate and effectively enriched DupA and DupB. This verified the applicability of the native probe to a complex proteome, showcasing that concerns related to enzymatic processing of the guanidium bond or the probe being an anomeric mixture are not significant issues.

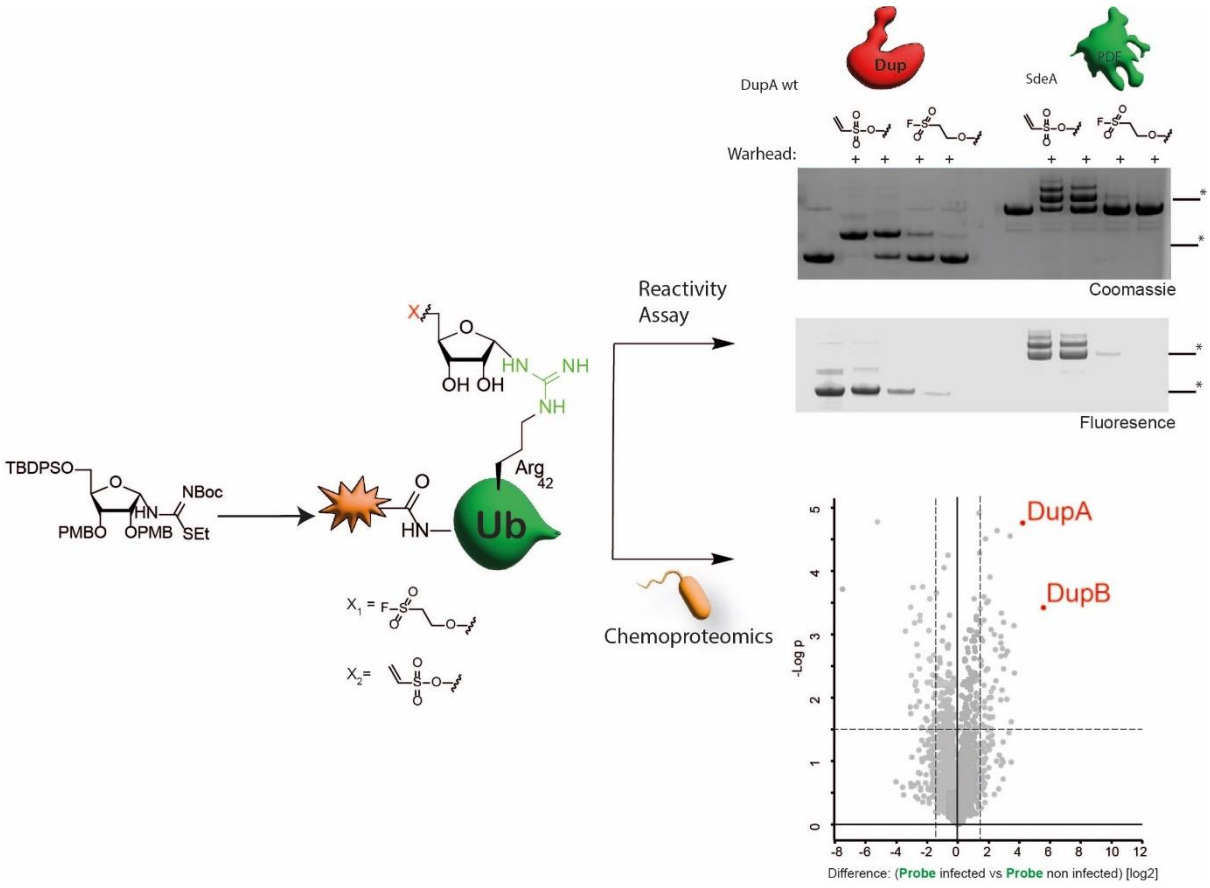

**Fig. 5**. Schematic representation of the work described in **Chapter 5**.

**Chapter 6** describes the development of a fluorogenic assay based on the reactive cysteine near the active site in DupA. A fluorogenic probe was synthesized by conjugating $Ub_{1-76}$ Arg42 → azidohomoalanine to an alkyne equipped methacrylamide-coumarin reagent via CuAAC. This compound specifically reacted with Cys196 of DupA inducing an addition-elimination reaction to release 7-hydroxycoumarin resulting in an increase of fluorescence intensity (FI) (**Fig. 6**). Interestingly, reacting the fluorogenic probe with the Legionella effector SdeA also resulted in an increase in FI. Although the targeted cysteine is a non-catalytic residue the location near the active site entrance might make this residue an interesting target for future drug development. The assay developed in this chapter can be applied in high-throughput screening campaigns to identify small molecule inhibitors of Dup/SidE activity.

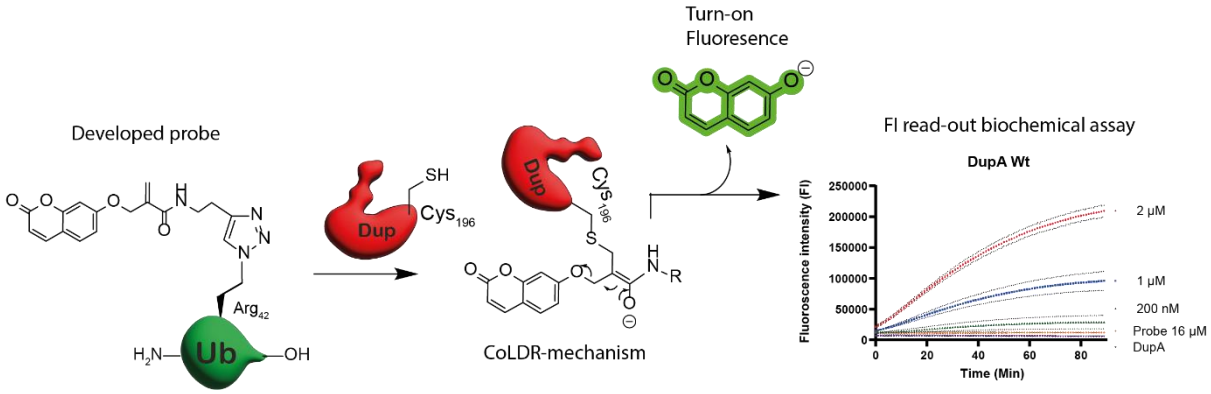


**Fig. 6**. Schematic overview of the work presented in **Chapter 6**.

In the final experimental chapter (**Chapter 7**), the focus shifts to $Ub^{ADPr}$ in mammalian cells, specifically investigating the Deltex (DTX) family of proteins. In DTX2, a RING E3 ligase, the RING domain is connected to a C-terminal Deltex (DTC) domain that binds ADPr. A recent study by Ahel and colleagues revealed that this RING-DTC fragment in DTX2 facilitates the ubiquitination of ADPr, attaching Ub to one of the secondary hydroxyls at the proximal adenosine part, leading to the formation of $Ub^{ADPr}$. In this study, the 3'-OH was pinpointed as the precise site of the ubiquitination event. In **Chapter 7**, two $Ub^{ADPr}$ mimics, where the ADPr moiety is linked to the 2' or 3' position, were synthesized as affinity probes. The synthesis was facilitated by equipping ADPr with a propargyl at one of the two hydroxyls and covalently conjugating this to ubiquitin with a C-terminally linked azide via CuAAC. Synthesis via this approach resulted in a non-native triazole linkage between Ub and ADPr. The probes were subjected to BLI measurements to assess their affinity to DTX2 (**Fig. 7**). Gratifyingly, both probes exhibited a $K_d$ in the low µM range, proving to be effective in binding DTX2. These probes hence can be used to explore novel $Ub^{ADPr}$ binders by performing a pulldown in cell lysate.

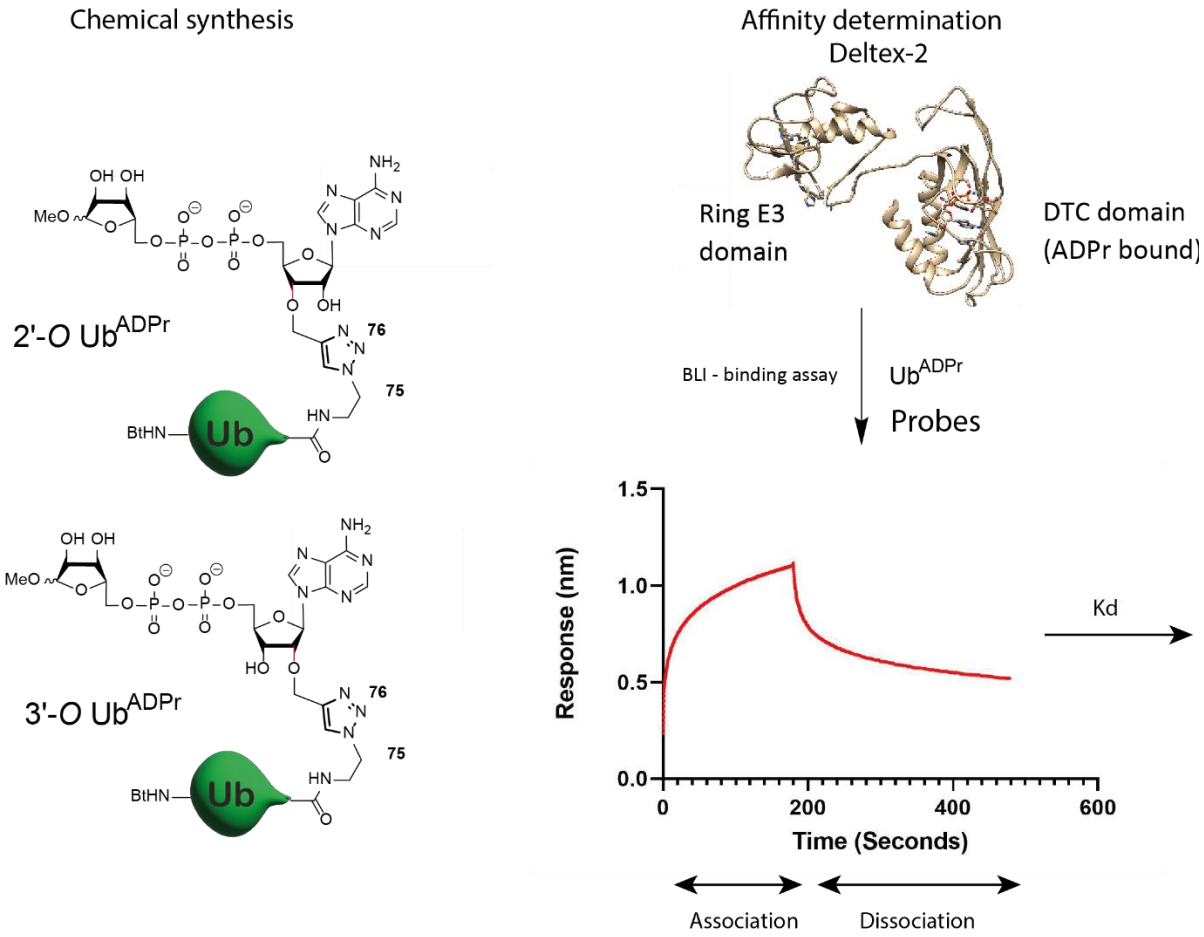


**Fig. 7**. Schematic overview of the work presented in **Chapter 7**.

## Future directions

### *SdeA and novel bacterial effectors*

In Chapter 5 we demonstrated the binding of the vinyl sulfonate probe to recombinant SdeA PDE. However, despite this demonstrated binding and high structural homology of PDE domains of SidEs to the Dups, the SidE effectors were not enriched by the vinyl sulfonate in the pulldown presented in Chapter 2. This may be attributed to the fact that the Legionella-infected cells in our study were lysed 4 hours post-infection. Previous research indicated that the activity of SdeA[7] is concentrated in the initial period after infection and is significantly reduced 4 hours post infection.[7] To elaborate on this, performing the pulldown at different time points, such as 1 hour post infection, would be of great interest as this could provide insights in the activity of these Legionella effectors at different times of infection.

Finding homologues of DupA and DupB in different (pathogenic) bacteria via bio-informatical searches is challenging due to the low sequence conservation of enzymes across prokaryotes. However, the probes presented in this thesis opens avenues to explore if these homologues exist via a chemical biology approach. This involves applying the covalent probes introduced in **Chapter 2** to intracellular replicating bacteria other than Legionella, for example *Shigella flexneri*, *Coxiella burnetii* and *Chromobacterium violaceum*. Interestingly, it is known that both pathogens introduce effectors that act on the host ubiquitin system upon infection.[8-11] Furthermore, the *Chromobacterium violaceum* utilizes CteC as mART to ADPribosylate ubiquitin on Thr-66 and this might indicate the bacterium also possesses PDE-effectors that ligate and reverse the conjugation of $Ub^{ADPr}$ to host substrates.[10,11] Applying the probes to different infected lysates could determine whether other pathogens exhibit such Dups, PDE domain-containing enzymes or interactors of $Ub^{ADPr}$, participating in pathways that exhibit similarities to the PR-ubiquitination pathway in *Legionella pneumophila*. This in theory could implicate a general mechanism of pathogens manipulating host systems and could serve as foundation to develop antibiotics treating multiple pathogen-induced infections. A feasible strategy to explore this seems to be performing pulldowns and additional chemoproteomics in the secretomes of pathogenic bacteria.

Additionally, it might be that bacterial effectors have distinct (Arg) recognition sites of Ub compared to DupA and DupB. To account for this, probes are synthesized installing the vinyl sulfonate warhead via a triazole linkage at all of the prospected Arg sites in biotinylated ubiquitin, via previously discussed methodology. This resulted in a library of ($Arg_X$ → triazole) site-variants **1-4** (synthesis described in **Supporting information**).

#### Beyond Arg – human $Ub^{ADPr}$ interactors

Mass-spectrometry experiments have established that in HeLa cell lysate, ubiquitin gets ADP-ribosylated on specific residues, namely Arg-42, Arg-54, Arg-74, Ser-20, Lys-6.[12] However, the proteins responsible for introducing and interacting with these different $Ub^{ADPr}$ analogues remain

to be identified. To explore this, pulldowns in mammalian lysate can be performed using either of the triazole-linked $Arg_x$ site variants (**1**-**4**), and the following proteomic analysis might identify potential interactors of Ub ADP-ribosylated on Arg-42, Arg-54 or Arg-74 (**Fig. 8**). Synthesizing the natively linked variants (Arg-42 (chapter 5), Arg-54 and Arg-74) and performing a similar chemoproteomic experiment might aid in validating the linkage specificity of protein interactors.

However, when exploring other ADPribosylation sites in Ub, such as Ser-20, the synthesis of a $^{Ser}Ub^{ADPr}$ conjugate would be challenging due to the acid sensitivity of the ester-linked glycosidic bond. For future exploration of $^{Ser}Ub^{ADPr}$ readers and writers, triazole-linked probes could be generated initially. These triazole linked probes might aid in identifying $^{ser}Ub^{ADPr}$ interactors via pulldown experiments. Subsequently, it might be necessary to develop novel chemistry to isolate native *O*-ADPr linked $Ub^{ADPr}$ which can then be used to validate if these protein interactors specifically recognize the native Ser-ADPr linkage in Ub.

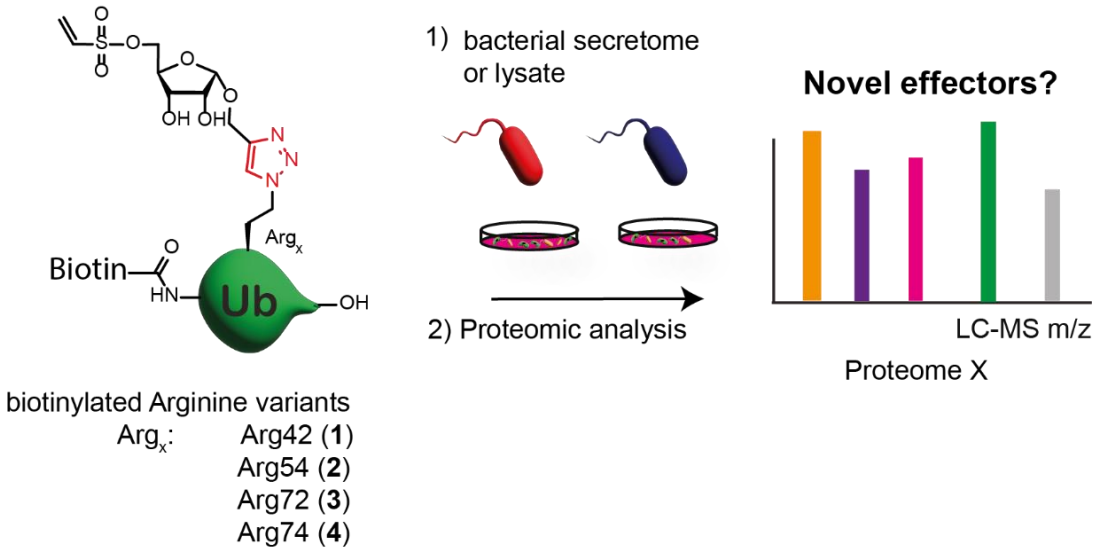


**Fig. 8.** Pulldown chemoproteomics workflow using biotin-vinyl sulfonate riboside $Ub_{76}$ probes (**1**-**4**) in the secretome or lysate of pathogenic bacteria.

### *Screening for allosteric covalent inhibitors – Cys196 of DupA*

Lately, allosteric covalent inhibitors are gaining interest, as demonstrated by the inhibition of the protein kinase Akt via covalently binding a non-catalytic cysteine.[13–15] In Chapter 2, the developed phosphoribose mimicking probe captured the non-catalytic Cys196 residue of DupA. Although the targeted cysteine is a non-catalytic residue, the location near the active site entrance might make this residue an interesting target for future drug development. The CoLDR-based assay (developed in chapter 6) to study allosteric binding to Cys-196 of DupA can be expanded to high-throughput screening (HTS) format and potentially might identify such covalent allosteric inhibitors. Furthermore exploring the potential of inhibiting catalytic activity via Cys196 modification, initial experiments using a bulky Ub-based probe or iodoacetamide indeed reduced catalytic activity, indicating potential for future small molecule binders to inhibit DupA activity.

The methacrylamide-Ub probe used in the CoLDR-assay generates a decent 11-fold increase in FI, however the reaction rate is moderate requiring 90 min of reaction time to reach this response. Before transitioning this assay to HTS format, it might be beneficial to optimize the probe, as using 2 µM of DupA and 16 µM of probe is a lot to be used in a screening. An optimized probe could enable the use of lower volumes and concentrations of probe to generate a same response. One strategy to accomplish this, is to improve the affinity by introducing ribose context in the molecule. This potentially reduces the equivalents of probe needed to get a proper FI read-out due to improved conversion. Converting the primary alcohol to an amine and introducing the methacrylamide warhead on this position in an anomeric alkyne equipped riboside would enable to furnish such a methacrylamide riboside Ub-based probe. The prospected synthesis is provided in **Scheme 1**. The synthesis is initiated, from mesylate **6**, a molecule previously prepared in chapter 2. A nucleophilic substitution treating **6** with sodiumazide afforded azide **7**. Subsequently, a straightforward Staudinger reduction converted the azide in amine **8** in 82% yield. The remaining part of the synthesis has to be executed in the future and entails a peptide coupling with methacrylamide coumarin carboxylic acid **9** to form **10**. Deprotection of the isopropylidine group and CuAAC using ubiquitin bearing an azide at position-42 in the sequence would furnish the probe, **12**.

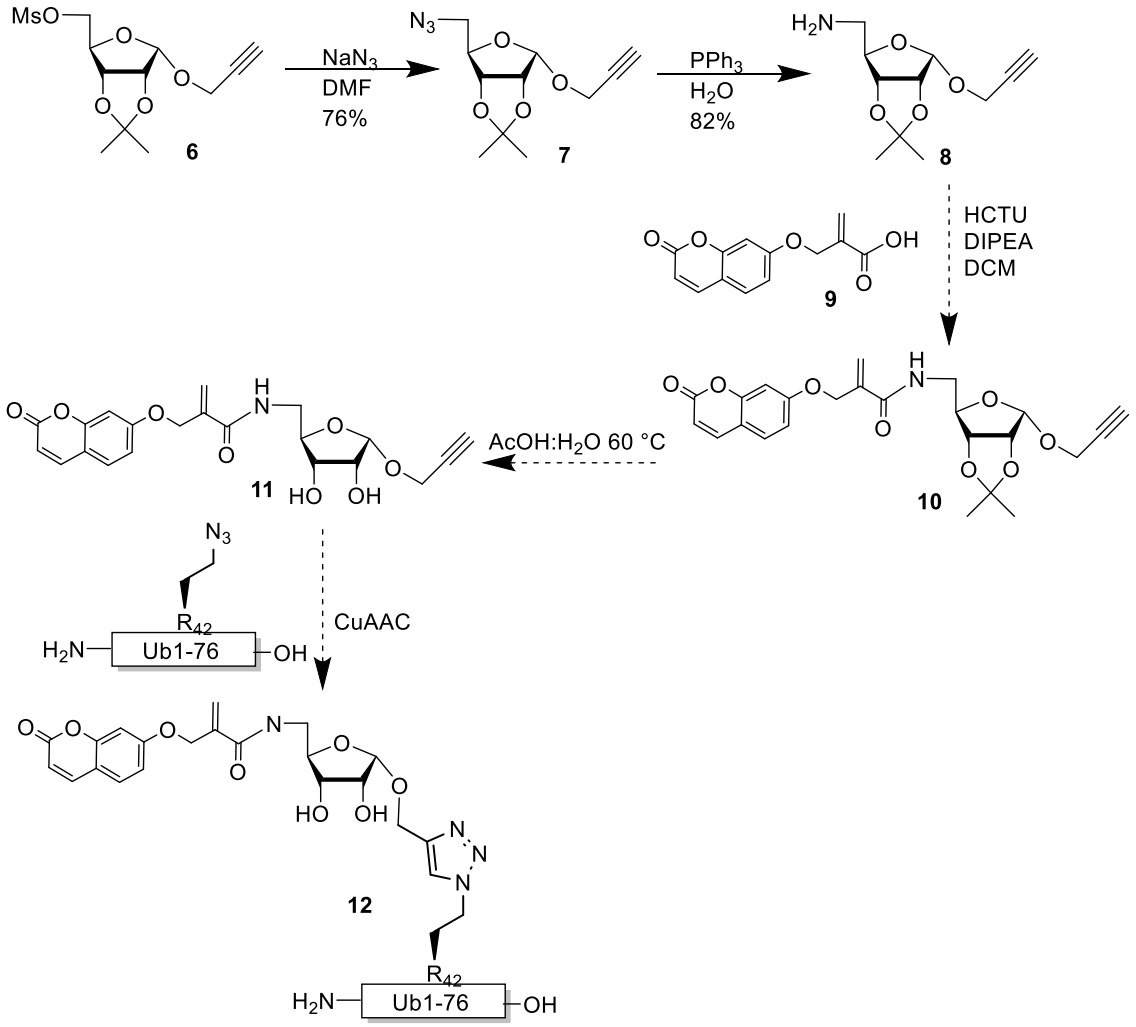


**Scheme 1**. Chemical synthesis route towards turn-on fluorescence probe **12**.

An alternative approach to improve the probe involves replacing the coumarin derivative with an adamantylidine-dioxetane-based chemiluminescent group. This functionality is known for its high signal-to-noise ratios reaching up to a 90-fold[19] increase (**Scheme 2**), and analogous probes are increasingly documented in literature.[16–21] To obtain a methacrylamide probe containing the chemiluminescent moiety, ribose **8** must be converted into an alkylating agent while containing the methacrylamide warhead as well. When established, an alkylation using this molecule and an adamantylidine-dioxetane-based reagent would follow. Starting from amine **8**, the acrylamide warhead is introduced via a peptide coupling using acrylic acid to yield **13**. Future synthesis, based on a procedure by Reddi *et al.*,[21] involves a Bayles-Hillman type reaction using 1,4-diazabicyclo[2.2.2]octane (DABCO) as nucleophilic catalyst to convert **13** into alcohol **14**, while preserving the acrylamide functionality. An Appel-reaction then can convert the alcohol into a bromide, generating riboside **15** as an alkylating agent. Alkylation with adamantylidine-dioxetane-based reagent **16** followed by deprotection of the isopropylidene affords **17**. In the final conjugation, CuAAC to ubiquitin possessing an azide at position-42 would form the "turn-on" chemiluminescent probe **18**. Via the CoLDR principle, the addition reaction of Cys196 in DupA

to the methacrylamide warhead would induce a subsequent elimination and liberate a phenolate-dioxetane intermediate. This intermediate then decomposes with the emission of a photon in the visible light spectrum. [18,21] If this chemiluminescent probe induces an improved fold-change compared to the coumarin-derivative this would enable to use lower concentrations of both enzyme and probe in HTS format.

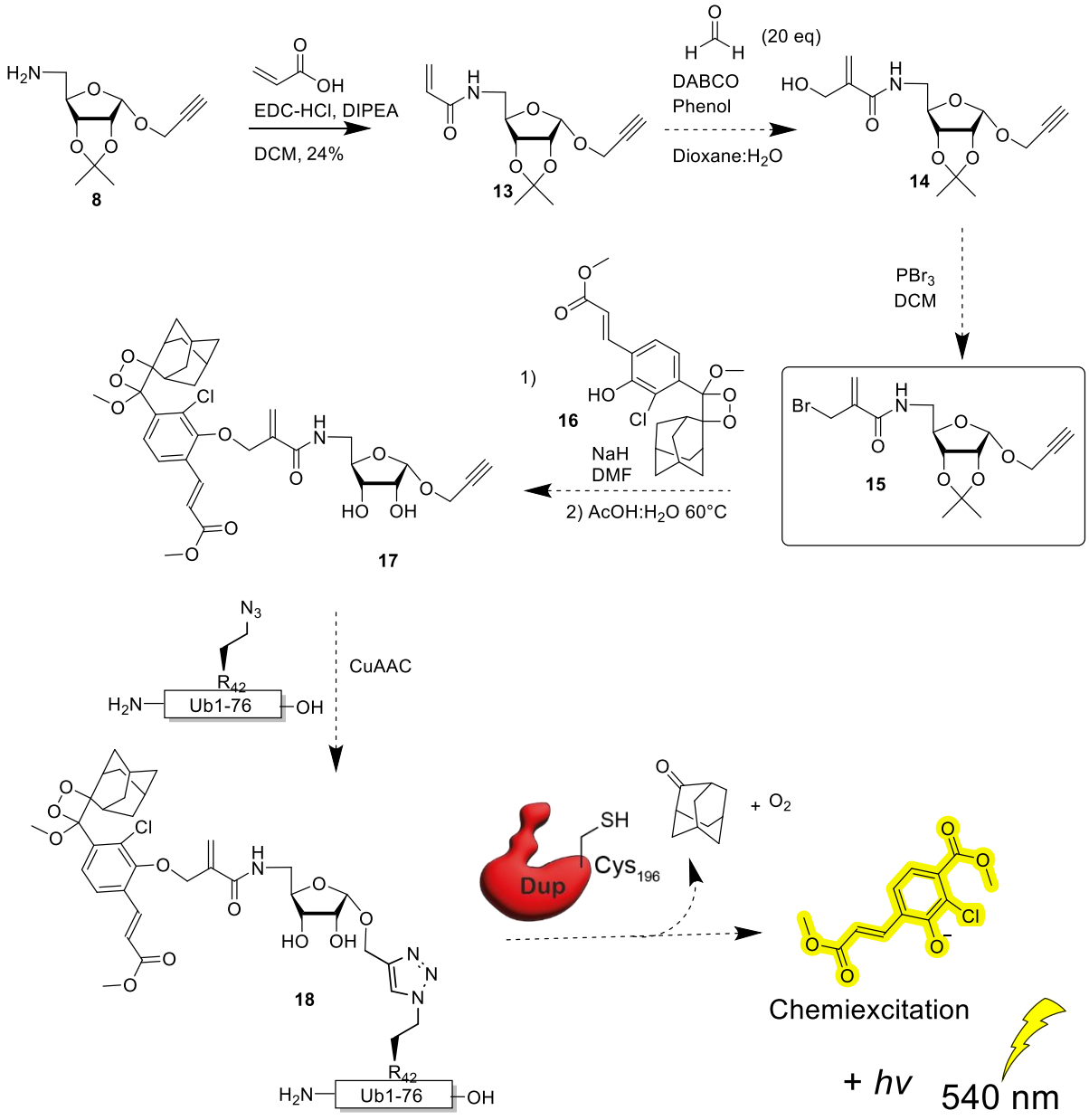


**Scheme 2**. A chemiluminescent probe **12** with potential improved signal to background ratio compared to the coumarin-based analogue.

### *(Activity-based) probes to study mammalian ADPr ubiquitinating enzymes*

The work in this dissertation described the development of affinity-probes to study the interaction between $Ub^{ADPr}$ and Deltex-2 (DTX2). The low µM affinity suggests suitability for conducting pulldown assays from lysate derived from mammalian cells to enrich for $Ub^{ADPr}$ interactors. This opens up a promising avenue for future research, as it can help identify potential mammalian enzymes that act on $Ub^{ADPr}$ and in a later stage could provide insights in the biological pathways involved. Another interesting future direction would be the covalent binding of the DTX enzymes, potentially achieved via activity-based probes (ABPs). The group of Ahel suggests the catalytic mechanism of the DTX enzyme relies on the deprotonation of one of the proximal adenosine secondary alcohol's in ADPr by a histidine residue.[22] Synthesizing an ADPr-analogue equipped with a (histidine) reactive warhead installed at the 2' or 3' of adenosine, such as a vinyl sulfonate could serve as an ABP. Such an ABP has the potential to covalently bind the active site His of DTX enzymes and in that case enables to monitor the activity of these enzymes under different cellular conditions, such as disease. Another potential feature of this probe would be to identify novel enzymes possessing a similar mode of action as the DTX enzymes. One potential ABP could be vinyl sulfonate **19**, which besides the warhead also contains a reporter molecule installed at the anomeric position (**Scheme 3**). The synthesis would be initiated from tri-acetylated riboside **20** and adenosine. In the case of a 3'-*O* warhead equipped ADPr the two crucial building blocks would be a 3'-*O*-vinylsulfonate phosphoramidite adenosine **21** and an 5'-O-Fm-protected phosphate containing an anomeric azide **22**. The two building blocks would be conjugated in a P(III)-P(V) coupling, oxidized and deprotected with TFA to obtain the $N_3$-ABP **23**. Throughout this thesis, it was found that the vinyl sulfonate warhead can withstand high percentages of TFA, making this acid-labile protecting group strategy feasible. The final ABP **19**, containing the His-reactive warhead and a reporter handle, would be obtained through CuAAC with a propargyl-variant of a reporter molecule. Incubating the ABP with recombinant DTX enzymes and their anticipated active site His mutants could confirm the formation of a covalent active site conjugate.

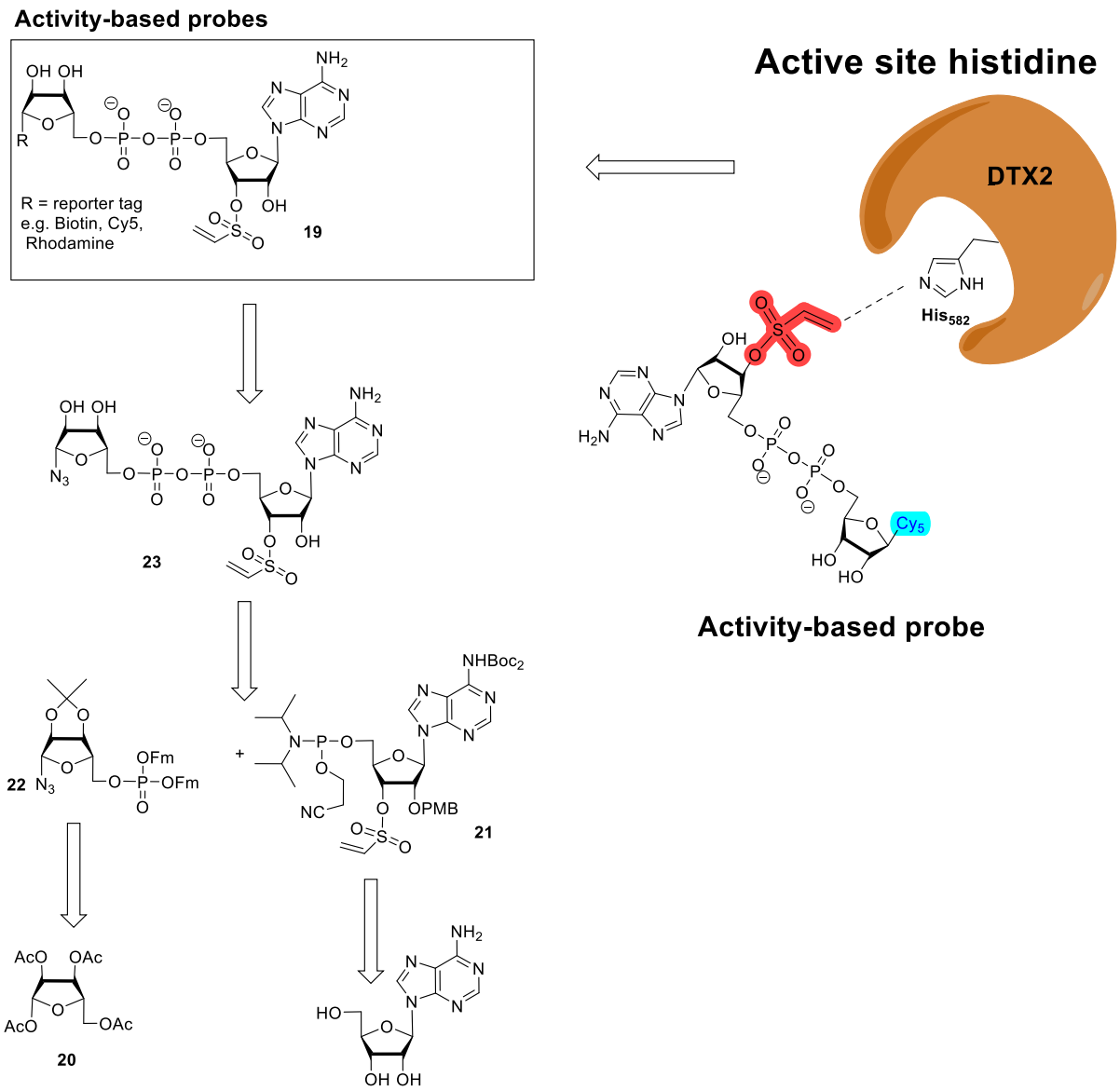


**Scheme 3**. Retrosynthesis of an activity-based probe to target His-582 of DTX2.

## References


1. Altmeyer, M. *et al.* Absence of poly(ADP-Ribose) polymerase 1 delays the onset of Salmonella enterica serovar typhimurium-induced gut inflammation. *Infect Immun* **78**, 3420–3431 (2010).

2. Bartlett, G. J., Porter, C. T., Borkakoti, N. & Thornton, J. M. Analysis of catalytic residues in enzyme active sites. *J Mol Biol* **324**, 105–121 (2002).

3. Tower, S. J., Hetcher, W. J., Myers, T. E., Kuehl, N. J. & Taylor, M. T. Selective Modification of Tryptophan Residues in Peptides and Proteins Using a Biomimetic Electron Transfer Process. *J Am Chem Soc* **142**, 9112–9118 (2020).

4. Zanon, P. R. A. *et al.* Profiling the Proteome-Wide Selectivity of Diverse Electrophiles. *Chemrxiv* (2021).

5. Liu, Q. *et al.* A General Approach Towards Triazole-Linked Adenosine Diphosphate Ribosylated Peptides and Proteins. *Angewandte Chemie* **130**, 1675–1678 (2018).

6. Kim, R. Q. *et al.* Development of ADPribosyl Ubiquitin Analogues to Study Enzymes Involved in Legionella Infection. *Chemistry - A European Journal* **27**, 2506–2512 (2021).

7. Kim, S., Isberg & R. R. The Sde Phosphoribosyl-Linked Ubiquitin Transferases protect the *Legionella pneumophila* vacuole from degradation by the host. *Proc Natl Acad Sci U S A* **120**, (2023).

8. Roberts, C. G., Franklin, T. G. & Pruneda, J. N. Ubiquitin-targeted bacterial effectors: rule breakers of the ubiquitin system. *EMBO J* **42**, (2023).

9. Qiu, J. & Luo, Z. Q. Legionella and Coxiella effectors: Strength in diversity and activity. *Nature Reviews Microbiology* **15**, 591–605 (2017).

10. Yan, F. *et al.* Threonine ADP-Ribosylation of Ubiquitin by a Bacterial Effector Family Blocks Host Ubiquitination. *Mol Cell* **78**, 641-652 (2020).

11. Tan, J. *et al.* Molecular basis of threonine ADP-ribosylation of ubiquitin by bacterial ARTs. *Nat Chem Biol* (2023).

12. Buch-Larsen, S. C. *et al.* Mapping Physiological ADP-Ribosylation Using Activated Ion Electron Transfer Dissociation. *Cell Rep* **32**, (2020).

13. Uhlenbrock, N. *et al.* Structural and chemical insights into the covalent-allosteric inhibition of the protein kinase Akt. *Chem Sci* **10**, 3573–3585 (2019).

14. Weisner, J. *et al.* Kovalent-allosterische Kinase-Inhibitoren. *Angewandte Chemie* **127**, 10452–10456 (2015).

15. Quambusch, L. *et al.* Covalent-Allosteric Inhibitors to Achieve Akt Isoform-Selectivity. *Angewandte Chemie* **131**, 18999–19005 (2019).

16. An, R., Wei, S., Huang, Z., Liu, F. & Ye, D. An Activatable Chemiluminescent Probe for Sensitive Detection of Î³-Glutamyl Transpeptidase Activity in Vivo. *Anal Chem* **91**, 13639–13646 (2019).

17. Hananya, N., Eldar Boock, A., Bauer, C. R., Satchi-Fainaro, R. & Shabat, D. Remarkable Enhancement of Chemiluminescent Signal by Dioxetane-Fluorophore Conjugates: Turn-ON Chemiluminescence Probes with Color Modulation for Sensing and Imaging. *J Am Chem Soc* **138**, 13438–13446 (2016).

18. Hananya, N. & Shabat, D. Recent Advances and Challenges in Luminescent Imaging: Bright Outlook for Chemiluminescence of Dioxetanes in Water. *ACS Cent Sci* **5**, 949–959 (2019).

19. Son, S. *et al.* Chemiluminescent Probe for the In Vitro and In Vivo Imaging of Cancers Over-Expressing NQO1. *Angewandte Chemie* **131**, 1753–1757 (2019).

20. Ye, S. *et al.* A Highly Selective and Sensitive Chemiluminescent Probe for Real-Time Monitoring of Hydrogen Peroxide in Cells and Animals. *Angewandte Chemie - International Edition* **59**, 14326–14330 (2020).

21. Reddi, R. N. *et al.* Tunable Methacrylamides for Covalent Ligand Directed Release Chemistry. *J Am Chem Soc* **143**, 4979–4992 (2021).

22. Zhu, K. *et al*. DELTEX E3 Ligases Ubiquitylate ADP-Ribosyl Modification on Protein Substrates. *Sci. Adv.* **8**, 4253-4270 (2022)

# Supporting information

### General synthetic procedures

All reagents were used as received unless stated otherwise. Solvents used in synthesis were dried and stored over 4Å molecular sieves, except for MeOH and MeCN which were stored over 3Å molecular sieves. Triethylamine (TEA) and diisopropylethylamine (DIPEA) were stored over KOH pellets. Column chromatography was performed on silica gel 60 Å (40-63 µm, Macherey-Nagel). TLC analysis was performed on Macherey-Nagel aluminium sheets (silica gel 60 $F_{254}$). TLC was used to visualize compounds by UV at wavelength 254 nm and by spraying with either cerium molybdate spray (25 g/L $(NH_4)_6Mo_7O_{24}$, 10 g/L $(NH_4)_4Ce(SO_4)_4{\cdot}H_2O$ in 10% $H_2SO_4$ water solution) or $KMnO_4$ spray (20 g/L $KMnO_4$ and 10 g/L $K_2CO_3$ in water) followed by charring at c.a. 250 $^oC$. NMR spectra were recorded on a Bruker AV-300 NMR. Chemical shifts (δ) are given in ppm relative to tetramethyl silane. Coupling constants (*J*) are given in Hz. All given $^{13}C$-APT spectra are proton decoupled.

### LC-MS measurements and HPLC purifications

LC-MS measurements were conducted on a Waters ACQUITY UPLC H-class System equipped with a Waters ACQUITY Quaternary Solvent Manager (QSM), Waters ACQUITY UPLC Photodiode Array (PDA) eλ Detector (λ = 210-800 nm), Waters ACQUITY UPLC Protein BEH C18 column (1.7 µM, 2.1 x 50 mm) and LCT Premier Orthogonal acceleration Time of Flight Mass Spectrometer (m/z = 100-1600) in ES+ mode. Samples were run for 3min at 40 °C using 2 mobile phases: A: MQ + 0.1% formic acid, B: MeCN + 0.1% formic acid. Gradient: 0 - 95% B at a flow rate of 0.5 mL/min. Data processing was performed using Waters MassLynx Mass Spectrometry Software 4.1 (deconvolution with MaxEnt1 function).

HPLC purification was performed on a **A)** Shimadzu semi-preparative RP-HPLC system, equipped with a Waters C18-Xbridge 5 µm OBD (10 x 150 mm) column at a flowrate of 6.5 mL/min. using 2 mobile phases: A: MQ + 0.05% FA, B: MeCN + 0.05 % FA. Gradient: 10 -> 70% B. HPLC system **B**) Waters preparative RP-HPLC system, equipped with a Waters C18-Xbridge 5 µm OBD (30 x 150 mm) column at a flowrate of 37.5 mL/min using 3 mobile phases: A: MQ, B: $CH_3CN$ and C: 1% TFA in MQ. Gradient: 20 -> 45% B, 5% C. High resolution mass spectra were recorded on a Waters XEVO-G2 XS Q-TOF mass spectrometer equipped with an electrospray ion source in positive mode (source voltage 3.0 kV, desolvation gas flow 900 L/hr, temperature 250 °C) with resolution R = 22000 (mass range m/z = 50-2000) and 200 pg/µL Leu-Enk (m/z = 556.2771) as a "lock mass".

General procedure **A**: Synthesis of biotinylated vinyl sulfonate $Ub_{76}$ probes **1**-**4**

$Arg_{\mathbf{x}}$ → azido homoalanine modified biotin-$(PEG_2)_2$ $Ub_{76}$ ($M + H^+$ = 9034, 4 mg, 0.44 µmol, 1 eq) was dissolved in DMSO (50 µL) and diluted in $H_2O$ (450 µL). This solution was added to TRIS buffer (1.5 mL, 20 mM TRIS/150 mM NaCl, pH 6.3) followed by the addition of vinyl sulfonate riboside **5** (described as compound **20** in chapter 2, 10 µL, 0.15M in DMSO, 1.5 µmol, 3.4 eq). To start the reaction 15 µL of freshly prepared click-mixture (1:1:1 v/v/v, $CuSO_4$ (100 mM in $H_2O$): Sodium Ascorbate (600 mM in $H_2O$): TBTA ligand (100 mM in MeCN) was added. The reaction mixture was shaken at 37 °C for 2 hours before LC-MS verified complete conversion to the product

(Deconvoluted mass found: (M + $H^+$ = 9312). The conjugate was purified by RP-HPLC and pure fractions were pooled and lyophilized.

Biotin-$(PEG_2)_2$-$Ub_{76}$ (Arg42 → triazole linked vinyl sulfonate ribose) (**1**)

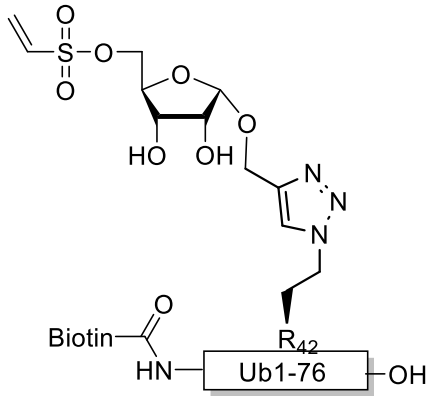


(Arg42 → vinyl sulfonate ribose) $Ub_{76}$ was synthesized following general procedure **A**. The CuAAC reaction was performed using Arg42 → azido homoalanine modified biotin-$(PEG_2)_2$-$Ub_{76}$ (M + $H^+$ = 9034, 4 mg, 0.44 µmol, 1 eq.) and **5** (10 µL, 0.15M in DMSO, 1.5 µmol, 3.4 eq.) to afford conjugate **1** as a white powder (1.54 mg, 0.17 µmol, 38% yield). Deconvoluted mass: (M + $H^+$ = 9312).

Biotin-$(PEG_2)_2$-$Ub_{76}$ (Arg54 → triazole linked vinyl sulfonate ribose) (**2**)

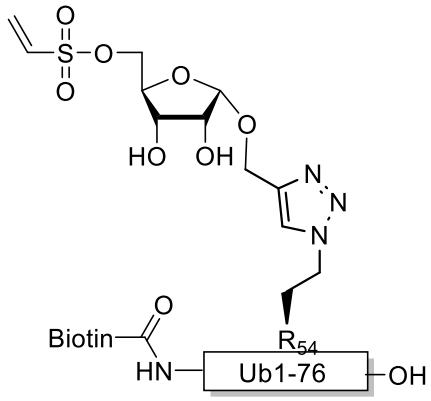


(Arg54 → vinyl sulfonate ribose) $Ub_{76}$ was synthesized following general procedure **A**. The CuAAC reaction was performed using Arg54 → azido homoalanine modified biotin-$(PEG_2)_2$-$Ub_{76}$ (M + $H^+$ = 9034, 4 mg, 0.44 µmol, 1 eq.) and **5** (10 µL, 0.15M in DMSO, 1.5 µmol, 3.4 eq.) to afford conjugate **2** as a white powder (1.1 mg, 0.12 µmol, 27% yield). Deconvoluted mass: (M + $H^+$ = 9312).

Biotin-$(PEG_2)_2$-$Ub_{76}$ (Arg72 → triazole linked vinyl sulfonate ribose) (**3**)

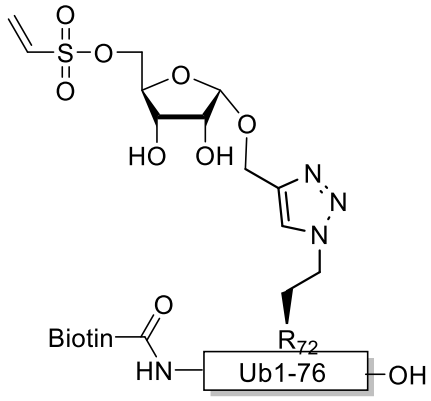


(Arg72 → vinyl sulfonate ribose) $Ub_{76}$ was synthesized following general procedure **A**. The CuAAC reaction was performed using Arg72 → azido homoalanine modified biotin-$(PEG_2)_2$-$Ub_{76}$ (M + $H^+$ = 9034, 4 mg, 0.44 µmol, 1 eq.) and **5** (10 µL, 0.15M in DMSO, 1.5 µmol, 3.4 eq.) to afford conjugate **3** as a white powder (1.2 mg, 0.13 µmol, 29% yield). Deconvoluted mass: (M+$H^+$ = 9312).

Biotin-$(PEG_2)_2$-$Ub_{76}$ (Arg74 → triazole linked vinyl sulfonate ribose) (**4**)

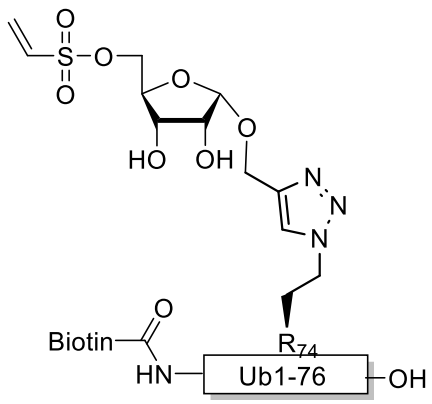


(Arg74 → vinyl sulfonate ribose) $Ub_{76}$ was synthesized following general procedure **A**. The CuAAC reaction was performed using Arg74 → azido homoalanine modified biotin-$(PEG_2)_2$-$Ub_{76}$ ($M + H^+ = 9034$, 4 mg, 0.44 µmol, 1 eq.) and **5** (10 µL, 0.15M in DMSO, 1.5 µmol, 3.4 eq.) to afford conjugate **4** as a white powder (1.38 mg, 0.15 µmol, 34% yield). Deconvoluted mass: ($M + H^+ = 9312$).

α-1-O-Propargyl-2',3'-*O-iso*propylidene-5'-O-azide-ribofuranose (**7**)

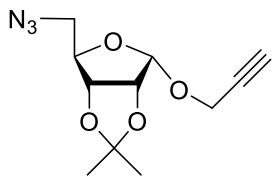


Ribose **6** (724 mg, 2.41 mmol) was co-evaporated with toluene and placed under $N_2$ atmosphere before dissolved in anhydrous DMF (8 mL). Subsequently, $NaN_3$ (313 mg, 4.82 mmol, 2 eq.) was added at the reaction stirred at 80 °C. After 15 min TLC indicated full conversion and the mixture was concentrated *in vacuo*. The residue was taken up in EtOAc and washed with $H_2O$ and brine. The organic layers was dried by $MgSO_4$ before concentrated in *vacuo*. Silica column chromatography (0 → 60% EtOAc in Heptane) obtained the azide **7** (463 mg, 1.82 mmol, 76% yield) as a colorless oil. $^1$H NMR (300 MHz, $CDCl_3$) δ 5.23 (d, *J* = 4.4 Hz, 1H), 4.72 (dd, *J* = 7.1, 4.5 Hz, 1H), 4.55 (dd, *J* = 7.1, 3.4 Hz, 1H), 4.39 – 4.27 (m, 2H), 4.29 – 4.22 (m, 1H), 3.58 – 3.32 (m, 2H), 2.41 (t, *J* = 2.4 Hz, 1H), 1.54 (s, 3H), 1.32 (s, 3H). $^{13}$C NMR (75 MHz, $CDCl_3$) δ 116.0, 99.7, 81.0, 81.0, 80.5, 78.9, 74.8, 54.9, 52.4, 26.0, 25.9.

α-1-O-Propargyl-2',3'-*O-iso*propylidene-5'-amine-ribofuranose (**8**)

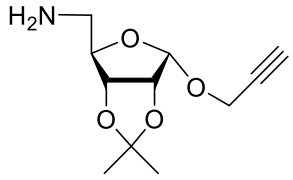


Ribose **7** (100 mg, 0.39 mmol) was co-evaporated with toluene, placed under argon atmosphere and dissolved in anhydrous THF (3.95 mL, 0.1M). Triphenylphospine (124 mg, 0.47 mmol, 1.2 eq.) was added and the reaction stirred at 40 °C. After 3 hours of stirring, $H_2O$ (1 mL) was added and the temperature increased to 60 °C. The reaction was stirred overnight before concentrated *in vacuo*. Silica column chromatography (0 → 5% MeOH in DCM) obtained the amine **8** (73 mg, 0.32 mmol, 82% yield) as a colorless oil. $^1$H NMR (300 MHz, MeOD) δ 5.18 (d, *J* = 4.4 Hz, 1H), 4.74 (dd, *J* = 7.2, 4.4 Hz, 1H), 4.56 (dd, *J* = 7.1, 3.4 Hz, 1H), 4.38 – 4.25 (m, 2H), 4.16 – 4.05 (m, 1H), 2.86 (t, *J* = 2.4 Hz, 1H), 1.52 (s, 3H), 1.34 (s, 3H). $^{13}$C NMR (75 MHz, MeOD) δ 116.9, 100.6, 83.1, 82.6, 82.1, 80.1, 75.9, 55.3, 44.2, 26.3, 26.1.

α-1-O-Propargyl-2',3'-*O-iso*propylidene-5'-acrylamide-ribofuranose (**9**)

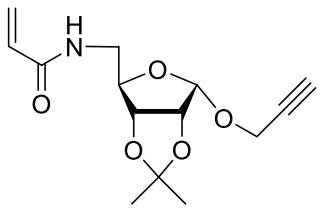

To a stirring solution of acrylic acid (27 µL, 0.40 mmol, 1.5 eq.) in anhydrous DCM (0.65 mL) were added EDC-HCl (75 mg, 0.40 mmol, 1.5 eq.) and DIPEA (70 µL, 0.40 mmol, 1.5 eq.). Thereafter, the amine **8** (60 mg, 0.26 mmol) in DCM (0.65 mL) was added dropwise at 0 °C and the reaction was subsequently allowed to reach rt. After stirring overnight, $H_2O$ was added and the aqueous layer extracted with DCM. Silica column chromatography (0 → 100% EtOAc in heptane) obtained the acryl amide **9** (18 mg, 0.06 mmol, 24% yield) as a colorless oil. $^1$H NMR (300 MHz, $CDCl_3$) δ 6.30 (dd, *J* = 16.9, 1.5 Hz, 1H), 6.10 (dd, *J* = 17.0, 10.2 Hz, 1H), 5.92 (s, 1H), 5.67 (dd, *J* = 10.2, 1.5 Hz, 1H), 5.20 (d, *J* = 4.4 Hz, 1H), 4.66 (dd, *J* = 7.2, 4.4 Hz, 1H), 4.48 (dd, *J* = 7.2, 3.6 Hz, 1H), 4.41 – 4.24 (m, 2H), 4.24 – 4.18 (m, 1H), 3.68 – 3.53 (m, 2H), 2.41 (t, *J* = 2.4 Hz, 1H), 1.54 (s, 3H), 1.32 (s, 3H). $^{13}$C NMR (75 MHz, $CDCl_3$) δ 165.8, 130.5, 127.3, 116.3, 99.4, 81.3, 81.0, 80.6, 79.1, 74.9, 54.9, 40.9, 26.1, 26.0.